

Research Article

MWCNTs/Resin Nanocomposites: Structural, Thermal, Mechanical and Dielectric Investigation**N. D. Alexopoulos^{1*}, E. P. Favvas^{2,*}, A.Vairis³ and A.Ch. Mitropoulos⁴**¹Department of Financial Engineering, University of the Aegean, Chios 821 32, Greece²Materials and Membranes for Environmental Separations Laboratory, Institute of Nanoscience and Nanotechnology, NCSR "Demokritos", Aghia Paraskevi, 153 41 Attica, Greece³Department of Mechanical Engineering, Crete Institute of Technology, Heraklion, 710 04, Greece⁴Hephaestus Laboratory, Department of Petroleum Mechanical Engineering, Eastern Macedonia and Thrace Institute of Technology, Ag. Loukas 654 04, Cavala, Greece

Received 5 November 2015; Accepted 18 November 2015

Abstract

Multi-wall carbon nanotubes (MWCNTs) were manufactured, characterized and added to a typical aeronautical resin matrix at different concentrations as nano-reinforcement. The carbon content of produced MWCNTs was determined to be around 98.5% while they consisted of 13-20 wall-layers and their external diameter had an average size in between 20 and 50 nm. MWCNTs were dispersed in an epoxy resin system and tensile specimens for different MWCNTs concentrations were prepared in an open mould. Electrical wiring was attached to the specimens' surface and surface electrical resistance change was in-situ monitored during monotonic tension till fracture. Performed tensile tests showed that the MWCNTs addition increased both modulus of elasticity and ultimate tensile strength on the nano-composites with a simultaneously dramatic ductility decrease. The MWCNTs addition enhanced the investigated resin matrix with monitoring ability; electrical resistance change of the investigated tensile tests was correlated in the elastic regime with axial nominal strain and the gauge factor of the different MWCNTs concentration specimens were calculated. It was found that lowest MWCNTs concentration gave the best results in terms of piezo-resistivity and simultaneously the least enhancement in the mechanical properties.

Keywords: Resin based materials, nanocomposite materials, carbon nanotubes, mechanical properties, thermal properties

1. Introduction

Both organic and inorganic materials became all-pervading as fillers in polymeric systems. Nowadays, many of composite polymer based materials are commercially available at various types of applications such as automobiles, aerospace components, building materials, marine architecture, sporting goods, textiles etc [1]. Nowadays needs for technological innovation pushes the research of composites to new products and enhancement in mechanical properties. For the development of nanocomposite materials at least one of the dimensions of the fillers must be in the in the size range from approximately 1 nm to 100 nm [2, 3]. Furthermore nanoparticles are these objects which have all three external dimensions at this scale [4]. It is within this range that materials can have substantially different properties compared to the same substances at larger sizes, both because of the substantially increased ratio of surface area to mass, and also because quantum effects begin to play a role at these dimensions, leading to significant changes in several types of physical property [3]. By adding these nanoparticles into the polymer matrix, the interactions between

nanoparticles and polymeric chains as well as between the nanoparticles themselves play an important role to the physicochemical properties of the novel materials [5]. In 1998 Oriakhi stating in the paper entitled "Nano sandwiches" [6]: "Nature is a master chemist with incredible talent. Using natural reagents and polymers such as carbohydrates, lipids, and proteins, nature makes strong composites such as bones, shells, and wood". So, bones, shells and wood are examples of natural nanocomposites materials, made from the mixing of two or more phases (i.e. particles, layers or/and fibers), where at least one of the phases is in the nanometer size range [7].

Numerous of nanomaterials have been reported as candidates for the preparation of nanocomposite polymer based materials. These derivative nanocomposites can be packaging materials, automotive parts, clothes, aircraft accessories and of course membranes. Some of them are natural products while many others are synthesized in the laboratory. From all these materials the most reported conventional and alternative fillers are the following: metal oxides [8], silica based materials [9], carbon molecular sieves [10], zeolites [11], layered silicates [12,13], carbon nanotubes [14,15], graphenes [16], clays [17,18], metal organic frameworks (MOFs) [19] etc. By using the above nanomaterials lighter but at the same time stronger material structures can be achieved. These nanocomposite materials simultaneously exhibit enhanced mechanical even electrical properties than their progenitors/precursor. Aerospace and

- E-mail address: nalexop@aegean.gr
 - E-mail address: e.favvas@inn.demokritos.gr
- ISSN: 1791-2377 © 2015 Kavala Institute of Technology. All rights reserved.

automotive industries are highly interest for this kind of nanocomposites.

More than 20 years ago in the central research laboratories of Toyota Usuki and co-workers reported a work where natural montmorillonite was used as filler material in Nylon-6 polymer matrix [20]. They found that just a small amount of nanofiller filling resulted in a notable improvement of both mechanical and thermal properties. From 1993 and up to date, the published articles in the field of preparation and characterization of nanocomposite polymer based materials can be easily found. The aim of the present article is to utilize multi wall carbon nanotubes as filler materials into commercial resin matrices. To this end, the physical and mechanical properties of the produced nanocomposite material depends not only on the properties of their individual parents (fillers and polymer matrix), but also on their morphology and interfacial characteristics [7,21,22].

Use of MWCNTs in polymers has attracted great attention due to their excellent mechanical and electrical properties [23]. Baron and Schulte [24] presented a methodology to monitor the surface / volume electrical resistance change of carbon fiber reinforced plastics during mechanical loading, due to the electrical capability of carbon fibers. Therefore, the addition of electrically conductive MWCNTs offers to non-conductive neat resins the potential for sensing capabilities through changes in electrical resistance on the onset of damage. Multi-walled carbon nanotubes (MWCNTs) exhibit high potential for an electrical modification of polymers because of their balanced properties and good process ability in terms of easy dispersion [25]. MWCNTs provided enhanced fracture properties [23] in polymer composites and could also serve another function, e.g. as a self-sensor. On the long run, they are expected to replace a number of sensors currently used in engineering structures for damage monitoring and sensing purposes and hence, lighter structures for lower fuel consumption will be achieved. Especially the self-sensing capability will primarily enhance safety and secondarily reduce the intervals of maintenance in such materials.

Research on these newly-developed, multi-functional materials is mainly focused on the enhancement of their mechanical performance as well as measurements of electrical resistance change simultaneously recorded from strain/stress variances of the testing specimens [26]. In the present work, MWCNTs additions will be attempted in a typical aeronautical epoxy matrix; microstructural, dielectric and mechanical characterizations will be performed. Different MWCNTs concentrations as reinforcement will be attempted in the epoxy resin system; microstructure and their physico/chemical properties will be investigated. Finally, their mechanical properties and their strain sensing capability will be evaluated.

2. Experimental Details

2.1. Materials

Multi-wall carbon nanotubes (MWCNTs) were synthesized using a novel catalytic chemical vapor deposition (CVD) technique. More specific, a fluidized bed chemical vapor deposition vertical reactor (FBCVD) which has been tailored for the synthesis of high-purity MWCNTs using proprietary catalysts was used [27-29]. Different MWCNTs concentrations per weight were added and dispersed in the

epoxy resin. A typical aeronautical epoxy resin Araldite LY564/hardener Aradur 2954 was used from Huntsman Advanced Materials, Bergkamen, Germany (ratio 100:35 parts by weight) as matrix in the present study.

2.2. Fabrication of the nanocomposites

A shear mixer was used in the present work to disperse the MWCNTs and to dissolve any formed agglomerates in the resinous matrix since it introduces high shear forces by a high speed rotating disc and the compound is stirred in a vacuum container to avoid air inclusions. Dispersion of MWCNTs in epoxy matrix had been performed via a Torus Mill™ dissolver (VMA, Getzmann GmbH). Dissolver's mixing time of the resin with the different percentages of CNTs, lasted more than 24 h each. The rotating disc was set at 4000 rpm for 180 min and the mixing was interrupted when the mixing chamber reached temperature higher than 30 °C. Four different MWCNTs concentrations were examined in the present article, namely 0.5, 1.0, 1.5 and 3.0 wt% of the resin matrix.

When mixing of the resin with the nano-reinforcement was over, then the resin was hand mixed with the catalyst (Aradur 2954 by Huntsman) and was placed on metallic moulds that had the shape of a typical tensile specimen, Fig. 1a. The tensile specimen dimensions were according to ASTM D 638, having a 50 mm gauge length at the reduced cross-section of the specimen. The manufactured specimens were thereafter cured for 2 hours at 60 °C followed by a 4 hour at 120 °C post cure, as recommended by the resin manufacturer's data sheet. The heat treatments were conducted in an electrical oven with ± 0.1 °C temperature control.

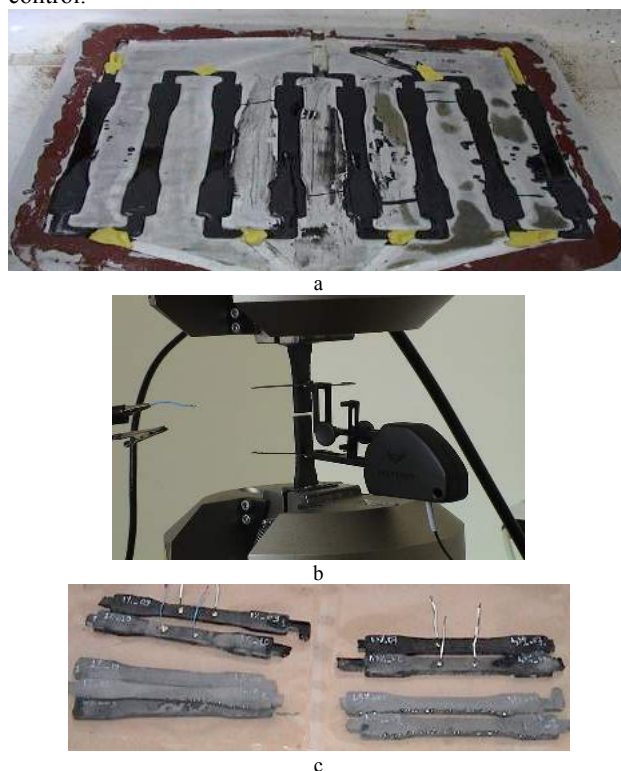


Fig. 1. (a) Open mould for the manufacturing of the resin specimens, (b) manufactured tensile specimens with varying MWCNTs concentration and attached cable connectors and (c) tensile specimen after fracture.

2.3. Characterization techniques

Both, MWCNTs and resin composite materials were characterized by several methods. X-ray diffraction (XRD) analysis was applied in the MWCNTs material in order to

detect the crystallinity and the kind of the carbon structure. The microscopic morphologies of the MWCNTs were evaluated by a scanning electron microscope (FE-SEM) at 30 kV, carried out on a JEOL-JSM-6390LV as well as by a JEOLJEM-2100F Transmission Electron Microscope (TEM). Thermal Gravimetric Analysis (TGA) was applied as a tool for the performance of the MWCNTs purity. Furthermore, resin/MWCNTs materials were also characterized, regarding their thermal stability, using a TGA/DTA–DSC Thermogravimetric/Differential Thermal Analyzer (Setaram, Setsys Evolution 18) using Argon as inert environment (50 ml/min), platinum crucibles, a heating rate of 5 °C and a sample mass of about 30 mg.

The thermal properties of the nanocomposite samples were also tested by differential scanning calorimetry (DSC) in a TA Instruments, Model MDSC 2920. Nitrogen was used as the purge gas to the DSC chamber at a rate of 50 ml/min during scans to prevent oxidation of the test sample. The

runs were undertaken using a heating ramp of 2 °C/min, a cooling rate of 5 °C/min with a temperature modulation of ± 0.32 °C every 60 s.

Wiring cables were attached to the surface of the tensile specimens at the gauge length (50 mm) with silver paste, Fig. 1b. A multimeter was used to record in situ the surface electrical resistance data of the specimen during mechanical testing. A DC voltage of 10 V was applied to cables connected to the specimens, the current was measured and the resistance was calculated from these values. The resistance measurements were performed in a two-point measurement set-up in the longitudinal direction. Data acquisition of 1 Hz was used for the resistance measurements and stored simultaneously in the P/C of the testing machine. A rubber mat was placed between the specimen and the metal grip of the test machine in order to insulate the specimen from the test machine.

Table 1. Experimental test matrix of MWCNTs nanocomposites.

	Percentage MWCNTs concentration (% wt) in resin matrix				
	0.0	0.5	1.0	1.5	3.0
Number of tensile specimens	14	10	7	8	9
Total					48

Tensile tests were performed according to the standard ASTM D638, using an MTS Insight electromechanical machine with maximum static load of 10 kN, Fig.1c. The displacement rate of the tensile machine grips was kept constant and equal to 0,016 mm/min. Initially, the two grips of the machine were aligned in order the specimen could not be twisted and suffer from parasitic bending loads. An Instron extensometer 2620-601 (50 mm gauge length) was attached on the reduced section of the specimen, to collect the accurate displacement data of the gauge length. During the experiments, force data, grips displacement as well as extensometer deformation were recorded and stored in a computer. In total almost 50 specimens were tensile tested; Table 1 shows the number of specimens tested per different MWCNTs concentration.

3. Results and Discussion

3.1. X-ray diffraction analyses of MWCNTs

The X-ray spectroscopy is a useful tool for the investigation/characterization of carbon structures. The powder XRD pattern (CuK α , $\lambda = 1.5406 \text{ \AA}$) of the multi-wall carbon nanotubes can be seen in Fig. 2. This spectrum exhibits a sharp (002) Bragg reflection at $2\theta \approx 26^\circ$ and is derived from the ordered arrangement of the concentric cylinders of graphitic carbon [30].

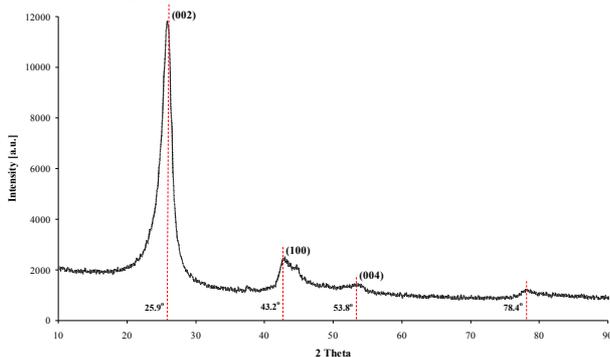


Fig. 2. XRD pattern of the investigated MWCNTs.

The “d-spacing” value corresponding to the (002) peak ($2\theta = 25.9^\circ$) was calculated at 3.44 \AA , a value which is very close to that of graphite (3.35 \AA) [31]. The presence of (002) peak in the XRD patterns suggests the multi-walled nature of carbon nanotubes. The pattern shows the main intense peak at $2\theta = 25.9^\circ$ and compared to the normal graphite ($2\theta = 26.5^\circ$), this peak shows a downward shift; which is attributed to an increase in the sp^2 , C=C layers spacing [32]. The second diffraction peaks can be noticed at the angle $2\theta \approx 43.2^\circ$ and indexed to the (101) reflection. In addition, two more meager peaks [33] were observed at 53.8° and 78.4° , the third and fourth reflexion of the main Bragg’s peak.

3.2. Morphology of MWCNTs and manufactured nanocomposites

Fig. 3 shows the SEM images of the purified MWCNTs that were used as nanofiller materials in the epoxy resin matrix. Only bundles of pure multi-wall carbon nanotubes can be observed and without any signs of impurities e.g., amorphous carbon. At the higher magnification picture, one can notice the ribbon type configuration of the MWCNTs. Finally, the diameter of MWCNTs was calculated to vary from 20 and up till 50 nm.

Transmission electron microscope images of the MWCNTs can be seen in Fig. 4; the existence of multi wall carbon nanotubes was observed, with an average size of the external diameter between about 20 and 50 nm. Overall, each carbon nanotube can be described as a tube with around 13 to 20 walls and an internal hole with the diameter size about the half of the MWCNTs external diameter size.

Scanning electron microscopy on the MWCNT reinforced resin revealed the formation of agglomerates; they consisted of high carbon nanotubes concentration and they were not sufficiently dispersed into the resin matrix. For all investigated MWCNTs reinforcements, it seems that the MWCNTs tend to form circular agglomerates and their size was measured to be approximate ranging from 1.1 to 2.5 μm . Fig. 5 shows a typical microstructure of the doped resin with 1.0 wt% MWCNTs as reinforcement. Carbon nanotubes were displayed as white circles and islands in the low

magnification image, while in the higher magnification images their microstructure can be noticed. The quantitative analysis in the last image confirmed the TEM analyses

results, showing that the MWCNTs diameter ranged from 40 to 60 nm.

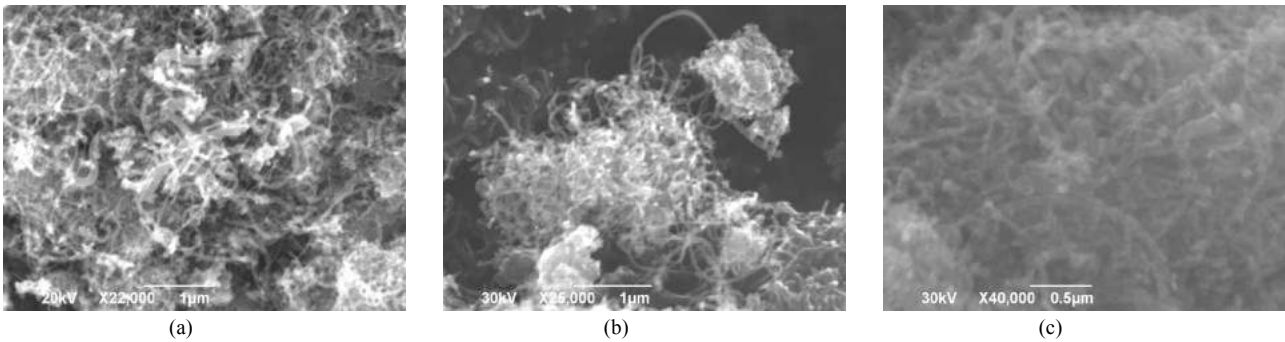


Fig. 3. SEM images of the investigated MWCNTs.

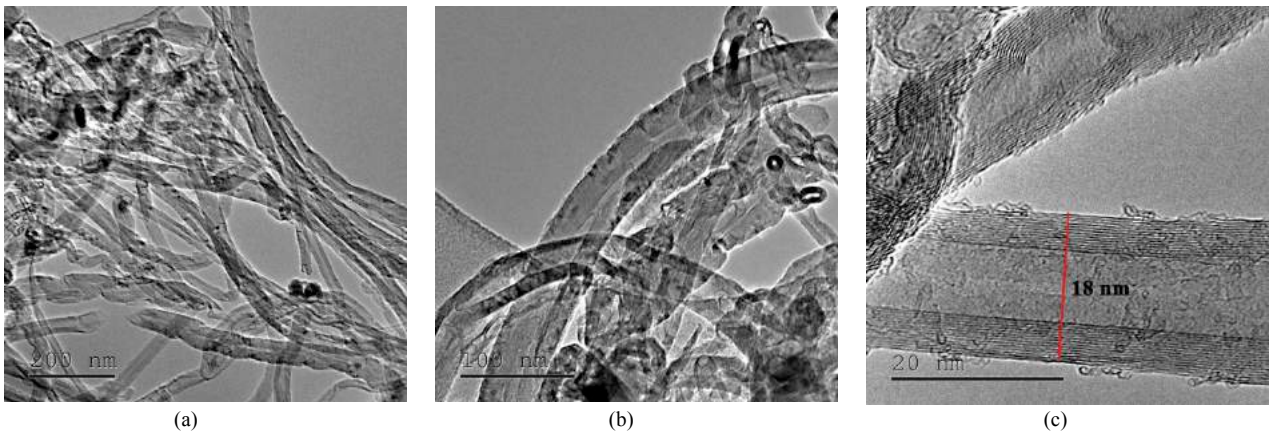


Fig. 4. TEM images of the investigated MWCNTs.

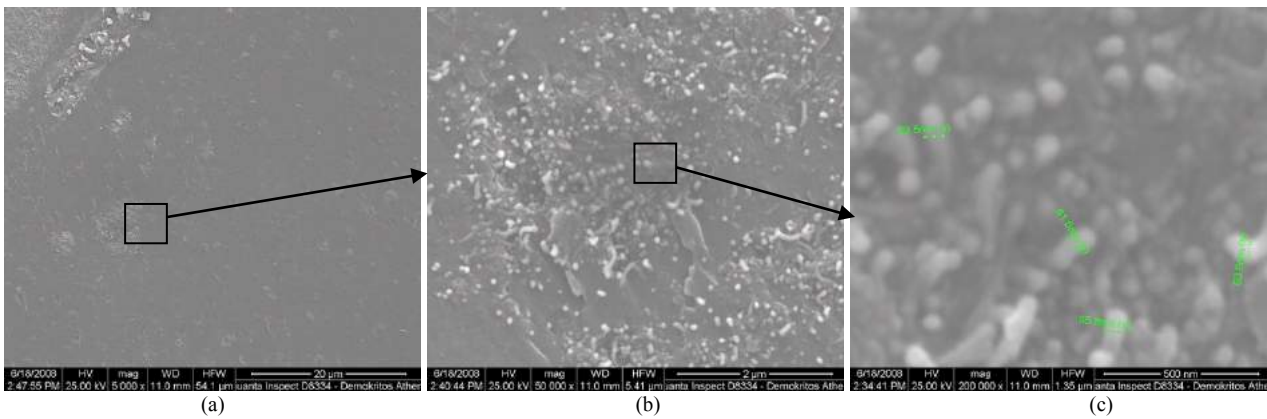


Fig. 5. SEM images of the nanocomposite resin with 1.0 wt% MWCNTs reinforcement

Respective results of the 3.0 wt% MWCNTs reinforcement in the resin matrix can be seen in Fig. 6. The highest doping percentage resulted again in the formation of agglomerates; the average diameter of the agglomerates was calculated with image analysis to be around 1.3 µm and they ranged from 0.3 to 2.2 µm. The agglomerate size was approximately the same with the previous percentage of MWCNTs doping, with the exception that more agglomerates were formed and dispersed within the matrix. Their shape is also circular to elliptical as noted in the specimens with the lower MWCNTs concentrations. Therefore, the only difference for the high MWCNTs concentration nanocomposite is the population of the

agglomerates. As the modulus of elasticity of the carbon nanotube is estimated to be of the order of 0.5 to 1 TPa, it is roughly estimated (by the simplistic rule of mixture) that the agglomerate might have globally an elasticity of the order of 100 GPa. Taking into account that the matrix has elasticity of the order of 2 GPa, this two times magnitude difference gives the impression that the agglomerates acts as rigid bodies within the “soft” resin matrix. Mechanics of materials show that in such cases nucleation of micro-cracking takes place at the interphase of the spheres and the matrix. The more elliptical their size is, the higher stress concentration at the interphase and therefore this essentially decreases their ductility and energy absorbing capacity capabilities.

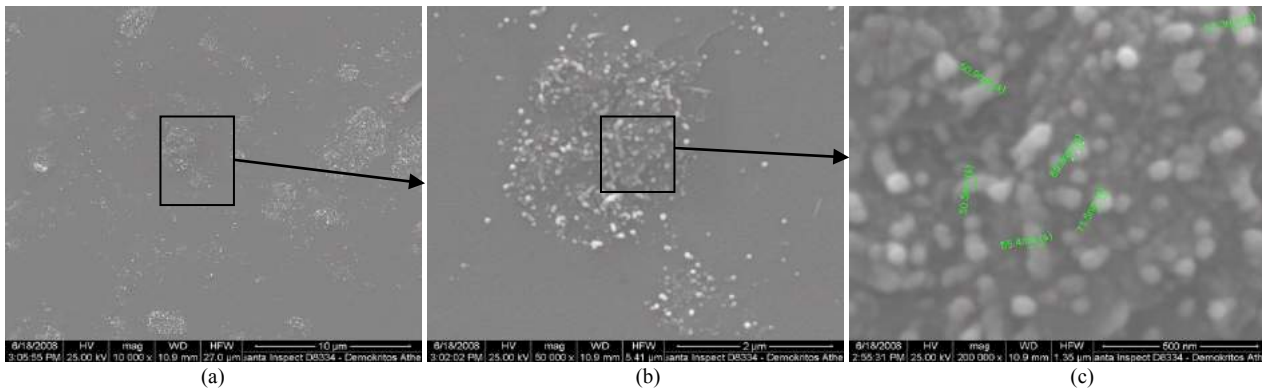


Fig. 6. SEM images of nanocomposite resin with 3.0wt% MWCNTs reinforcement

3.3. Thermal gravimetric analysis

All the samples were heated from ambient to 900 K in platinum crucibles, with the same heating rate of 5 °C/min. The oven was fed with 50 cm³/min pure Ar, while the heat flow rate was kept constant through out the pyrolysis process. Argon was chosen as a pyrolysis gas since it is considered to be the best non-active gas for polymeric precursor materials; it results to a mild activation action than it is possible to be performed with other gases such as helium or nitrogen [34].

The main weight loss zone was in between 585 and 800 K for all samples and the weight loss lies from 10 up to 96 %, Fig. 7. For higher temperatures above 850 K the samples became amorphous carbon structures and finally only the MWCNTs concentration remained in the crucible. As mentioned in Fig. 7, at temperatures up to ~650 K no “logical” behavior can be concluded regarding the ordering of the samples stability. This behavior is observed in the “logical” direction at temperatures higher than 650 K. Fig. 7 shows that the samples with higher MWCNTs concentration are more stable as the weight loss recorded less in the case of “MWCNT/Resin 3.0 wt%” sample and follows the samples with MWCNTs concentration of 1.5, 1.0, 0.5 wt%. Finally the higher amount of degraded weight corresponds to the pure resin material. In any case, both single phase resin material as well as nano-reinforced resins presented remarkable thermal properties and can be proposed as candidate materials at various applications in material manufacturing industry.

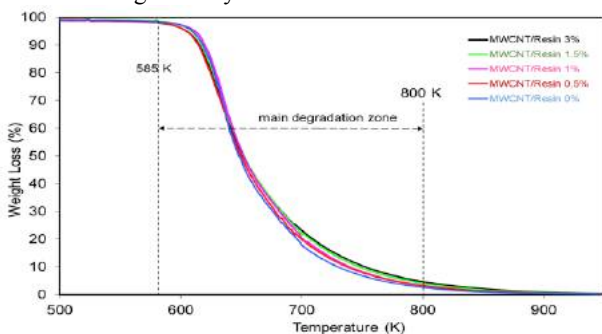


Fig. 7. TGA curves of the MWCNTs/resin nanocomposites at temperature up to 900 K.

3.4. Differential scanning calorimetry

Differential scanning calorimetry was used to study the purity, crystallinity and the grade of the homogenization of the two mixed phases of the nanocomposite materials, namely the MWCNTs and the resin matrix. The glass transition temperatures fluctuated from 387 to 400 K without

any sequence based on the filler concentration grade (Fig. 8a). In specific, 400, 394, 387 and 397 K were calculated to be the glass transition temperature T_g for the nanocomposites with MWCNTs concentration of 3.0, 1.0, 0.5 and 0.0 %wt, respectively. For the case of 1.5 wt% reinforced sample, the DSC curve didn't provide any characteristic region (inflection point) where T_g could be calculated. This is an argument that the two mixed phases didn't formed into a homogeneous final phase. Another evidence of the poor dispersion of the MWCNTs in the same sample is that in the DSC spectra; the main exothermic peak is split at two secondary, the first one at 579 and a second at 617 K. This happened since during the mixing stage of the carbon nanotubes with the resin, two separated phases probably phases with similar MWCNTs “concentration” and different crystallinity grade were formed. For the rest samples only one exothermic peak at around the 620 K can be observed and these peaks can be attributed to the melting process of the polymeric chains. The presence of broad endothermic peaks also confirmed the amorphous nature of the composite materials [35].

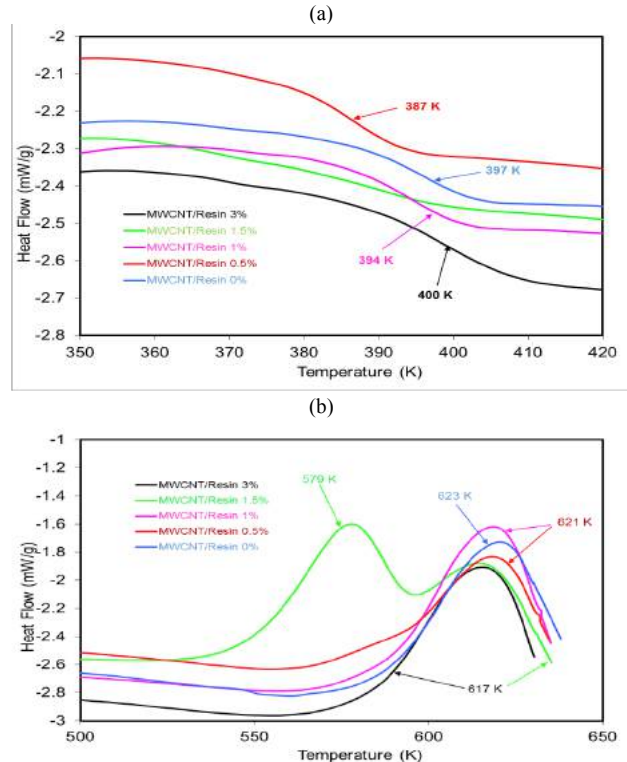


Fig. 8. DSC curves of the MWCNTs/resin nanocomposites at the temperature range of 500 - 660 K.

3.5. Mechanical properties

Tensile test results of the MWCNTs reinforced resins are summarized in Table 2. Modulus of elasticity E , tensile strength R_m and elongation to fracture A_T are plotted for the different investigated MWCNTs concentration in Fig. 9. As expected, the incorporation of the ‘hard’ MWCNTs to the

resin, fully dispersed or even with formed agglomerates in the resin’s microstructure is expected to increase the modulus of elasticity of the doped resin. Indeed, elasticity was increased from the 2.374 GPa of the neat resin to the value of 2.532 GPa for the highest MWCNTs concentration, which corresponds to an approximate 7 % increase.

Table 2. Evaluated tensile mechanical properties of the MWCNTs nanocomposites.

Mechanical property	Percentage MWCNTs concentration (% wt) in resin matrix				
	0.0	0.5	1.0	1.5	3.0
Modulus of elasticity E [GPa]	2.374 ± 0.161	2.417 ± 0.137	2.474 ± 0.105	2.511 ± 0.128	2.532 ± 0.149
Ultimate tensile strength R_m [MPa]	59.9 ± 12.6	62.1 ± 7.3	65.1 ± 8.9	67.0 ± 10.5	72.1 ± 5.8
Elongation to fracture A_T [%]	3.71 ± 1.08	2.71 ± 0.71	2.36 ± 0.32	2.27 ± 0.81	1.84 ± 0.26

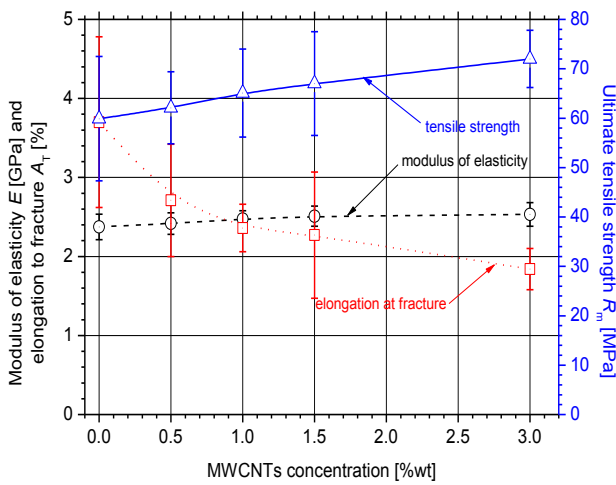


Fig. 9. Evaluated tensile test results of the MWCNT doped resins.

Despite this appreciable modulus of elasticity increase, evaluated tensile test results showed an essential trade-off in the tensile mechanical properties. For example, ultimate tensile strength R_m is increasing with decreasing elongation to fracture A_T (ductility) for the continuous increasing MWCNTs concentration. Ultimate tensile strength takes values above 70 MPa for the highest reinforced concentration and the R_m increase seems to be linear along with the concentration increase. This was not the case for ductility, as it seems to be exponentially decreasing with the small MWCNTs reinforcements (up to 1.0 %wt) and linear decreasing for higher concentrations.

The available tensile test results were plotted in Fig. 10 when normalized to the initial respective property of the reference (undoped) resin. This trade-off between strength and ductility can be quantitatively seen in Fig. 9; for the highest doping percentage of 3.0% MWCNTs an almost 20 % increase in tensile strength R_m values is followed by a dramatic decrease (almost 50 %) in ductility property A_T . The outcome of the above mechanical properties were more-or-less expected, since the rigid agglomerates within in the ‘soft’ resin acts as stress raisers and therefore premature fracture occurs; this quite describes the trade-off between strength and ductility in such materials.

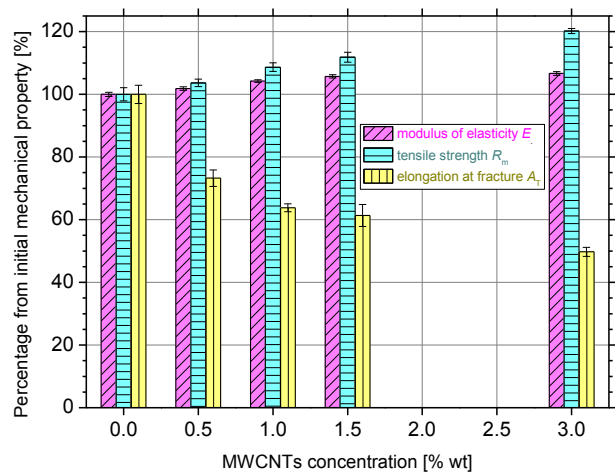


Fig. 10. Evaluated tensile test results of the MWCNT doped resins as percentages of the initial mechanical property.

3.6. Electrical properties

It is well known that the electrical properties can be expressed through the electrical resistance change (ERC) value of produced nanocomposites. The physical background of ERC values is strongly connected with the connections among MWCNTs as well as the tunneling effect when the carbon nanotubes are not in contact. Increasing ERC of the coupons with the increasing mechanical load can be translated as some MWCNTs are beginning to lose their common contact points or the distance between several MWCNTs is increasing and thus the tunneling effect is diminishing. Hence, the paths for the electrical current to pass are becoming less that quite increases the surface electrical resistance of the specimens.

Typical monotonic tensile engineering stress - strain curves in the elastic regime (approximately up to 40 MPa) and their simultaneously measured electrical resistance change (ERC) for three tensile specimens with different MWCNTs concentration can be seen in Fig. 11. As being in the elastic regime, tensile curves are absolutely linear; ERC increase is also almost linear with the monotonically increasing tensile stress for all specimens, especially within the regime up to 1.0 % axial strain. Exception is perhaps the 3.0 wt% specimen where this correlation is part linear part polynomial (or exponential). Globally from Fig. 11, it can be understood that both mechanical and electrical response of the nanocomposites varies with different MWCNTs concentration.

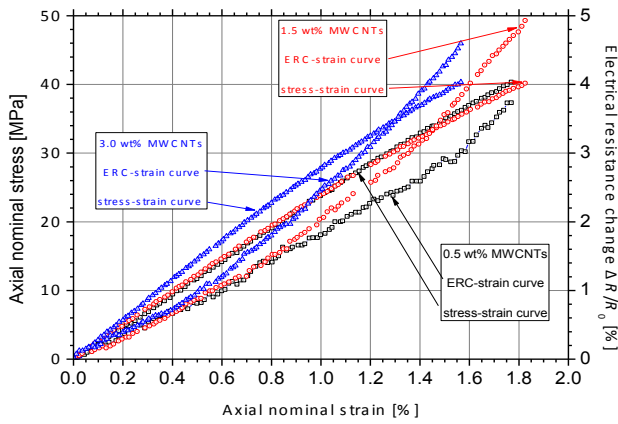


Fig. 11. Mechanical and electrical response to monotonic tension for different MWCNTs concentration specimens.

As one the goal of the present work is to incorporate MWCNTs for strain sensing purposes, the typical combined mechanical and electrical results were plotted in Fig. 12. ERC was plotted in the x-axis as it represents the readings from the sensor (surface electrical resistance change) and uniform axial strain in the y-axis (property to be prognosed). The results from three typical specimens with varying MWCNTs concentration can be seen in the figure as well as their linear approximations to fit the curves. It can be noticed that the slope of the fitting linear curves is continuously decreasing with increasing MWCNTs concentration. The resistance to strain (RS) coefficient (slope of the fitting linear) was calculated for the linear correlation between measured ERC ($\Delta R/R_0$) and axial strain, as:

$$strain = RS \cdot \left(\frac{\Delta R}{R_0} \right)$$

RS coefficient was found to be decreasing with increasing MWCNTs concentration from the initial value of 0.5182 for the 0.5 wt% MWCNTs specimens and up to the approximate value of 0.3779 for the 1.0 wt% MWCNTs specimens. RS actually represents the gauge factor for converting the ERC readings to axial strain measurements within the elastic regime of the specimen. All RS measurements for the investigated specimens were calculated as average values and standard deviation and can be seen in Fig. 13. An almost linear approximation ($R^2 = 0.95$) can be noticed for the measured gauge factor of the produced nanocomposites with varying MWCNTs concentration. For engineering applications, it would be preferable to have the highest screening of the applied strain by reading high values of electrical resistance change. Hence, the highest value of the gauge factor can be noticed for the lowest investigated concentration that is well-above the percolation threshold. Therefore, another trade-off was set in the investigated nanocomposites; the lowest MWCNTs concentration gave the best results in terms of sensing with the lowest enhancement in the mechanical properties, while the highest concentration gave absolutely the opposite. It is a matter of individual judgement to the design engineer to proceed with the lowest enhancement in mechanical properties of the newly-developed nano-reinforced resins.

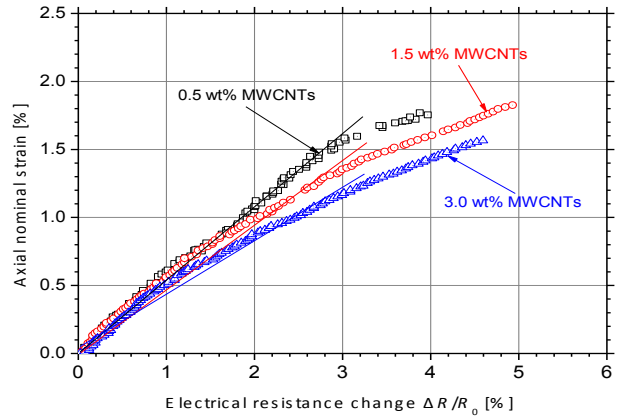


Fig. 12. Electrical resistance change over axial strain for different MWCNTs concentration specimens.

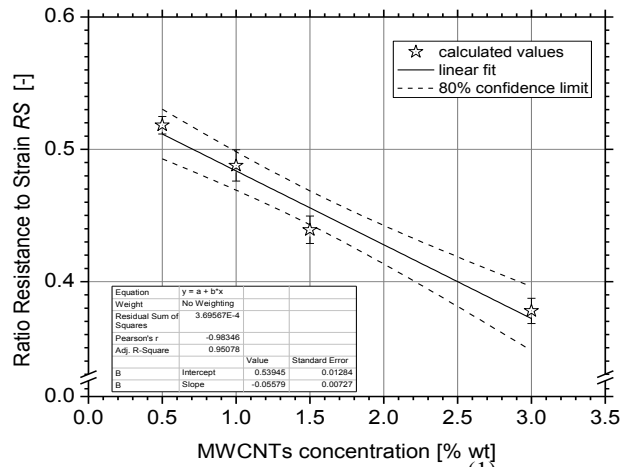


Fig. 13. Calculated resistance to strain values (gauge factor) of the investigated MWCNTs concentration specimens.

4. Conclusions

High purity MWCNTs were prepared via FBCVD process and were used as filler materials in resin based nanocomposite materials. The prepared carbon nanotubes had 13 to 18 wall-layers and presented homogeneity in their average dimensions. SEM images revealed that a small amount of not well dispersed carbon nanotubes were formatted in circular form of agglomerates of about 3 to 5 μm . Regarding their thermal properties, TGA revealed that the loading of higher amount of MWCNTs concluded on more stable nanocomposite materials. Furthermore, as the DSC convinces, all the nanocomposite materials had a clear T_g region between 394 and 400 K except the sample MWCNT/Resin 1.5 wt% which presented bad homogeneity between the two consisted phases.

Addition of MWCNTs at different concentrations enhanced the mechanical performance of the newly-developed nanocomposites. Modulus of elasticity and ultimate tensile strength was increased with increasing MWCNTs concentration while the opposite was noticed for elongation to fracture. Strain sensing ability was evaluated in the elastic regime of the tensile tests. Evaluated gauge factor (electrical resistance change to axial strain ratio) was calculated for all investigated specimens, showing that the lowest MWCNTs concentration gave the best results in terms of better screening the dielectric measurements. Therefore, a trade-off can be established between enhancement of mechanical properties and strain sensing

ability in terms of better screening the electrical measurements.

Acknowledgments

The authors gratefully acknowledge the financial support of the European Union (European Social Fund – ESF) and Greek national funds through the Operational Program "Education and Lifelong Learning" of the National Strategic

Reference Framework (NSRF) - Research Funding Program: "Archimedes III – Technological Educational Institute of Crete – Development of nanostructured materials with carbon nanotubes for use in high strength (transport) applications -NANOSTRENGTH".

The authors would like also to thank Dr. John W. Nolan for the SEM and TEM images of the produced MWCNTs.

References

1. Morgan, AB (2006) Flame retarded polymer layered silicate nanocomposites: a review of commercial and open literature systems. *Polym Adv Technol* 17:206–217.
2. Kreyling WG, Semmler-Behnke M, Chaudhry Q (2010) A complementary definition of nanomaterial. *Nano Today* 5:165–168.
3. Favvas, EP (2015) Chapter: "Nanomaterials and their applicability as membranes' fillers", in book entitled «Innovations in Nanomaterials», Nova Science Publishers, Inc., ISBN: 978-1-63483-548-0, New York, U.S.A.
4. Buzea C, Pacheco I, Robbie K (2007) Nanomaterials and nanoparticles: Sources and toxicity. *Biointerphases* 2:MR17–MR71.
5. Ozin GA, Arsenault A, Cademartiri L (2008) *Nanochemistry: A Chemical Approach to Nanomaterials: Edition 2*, The Royal Society of Chemistry (BOOK).
6. Oriakhi C (1998) Nano sandwiches. *Chemistry in Britain* 34:59–62.
7. Hussain F, Hojjati M, Okamoto M, Gorga RE (2006) Review article: Polymer-matrix Nanocomposites, Processing, Manufacturing, and Application: An Overview. *J. Compos. Mater.* 40:1511–1575.
8. Goh PS, Ismail AF, Sanip SM, Ng BC, Aziz M (2011) Recent advances of inorganic fillers in mixed matrix membrane for gas separation. *Separ Purif Technol* 81:243–264.
9. Aramendia MA, Borau V, Jimenez C, Marinas JM, Porras A, Urbano FJ (1996) Synthesis and characterization of various MgO and related systems. *J Mater Chem* 6:1943–1949.
10. Buonomenna MG, Yave W, Golemme G (2012) Some approaches for high performance polymer based membranes for gas separation: block copolymers, carbon molecular sieves and mixed matrix membranes. *RSC Adv* 2:10745–10773.
11. Bastani D, Esmaceli N, Asadollahi M (2013) Polymeric mixed matrix membranes containing zeolites as a filler for gas separation applications: A review. *J Ind Engin Chem* 19:375–393.
12. Deng H, Lin P, Xin S, Huang R, Li W, Du Y, Zhou X, Yang J (2012) Quaternized chitosan-layered silicate intercalated composites based nanofibrous mats and their antibacterial activity. *Carbohydr Polym* 89:307–313.
13. Shokuhfar A, Zare-Shahabadi A, Atai A-A, Ebrahimi-Nejad S, Termeh M (2012) Predictive modeling of creep in polymer/layered silicate nanocomposites. *Polym Test* 31:345–354.
14. Calvert P (1999) Nanotube composites: A recipe for strength. *Nature* 399:210–211.
15. Moniruzzaman M, Winey KI (2006) Polymer Nanocomposites Containing Carbon Nanotubes. *Macromolecules* 39:5194–5205.
16. Stankovich S, Dikin DA, Dommett GHB, Kohlhaas KM, Zimney EJ, Stach EA, Piner RD, Nguyen ST, Ruoff RS (2006) Graphene-based composite materials. *Nature* 442:282–286.
17. Usuki A, Hasegawa N, Kato M (2005) Polymer-Clay Nanocomposites. *Adv Polym Sci* 179:135–195.
18. Sapalidis AA, Katsaros FK, Romanos GE, Kakizis NK, Kanellopoulos NK (2007) Preparation and characterization of novel poly-(vinyl alcohol)-Zostera flakes composites for packaging applications. *Compos Part B-Eng* 38:398–404.
19. Zhu Q-L, Xu Q (2014) Metal-organic framework composites. *Chem Soc Rev* 43:5468–5512.
20. Usuki A, Kawasumi M, Kojima Y, Okada A, Kurauchi T, Kamigaito OJ (1993) Swelling Behavior of Montmorillonite Cation Exchanged for V-amino Acids by E-caprolactam. *Mater Res* 8:1174–1178.
21. Kanatzidis MG, Wu CG, Marcy HO, DeGroot DC, Kannewurf CR (1990) Conductive-Polymer/Bronze Nanocomposites. Intercalated Polythiophene in V2O5 Xerogels. *Chem Mater* 2:222–224.
22. Alubaidy A, Venkatakrisnan K, Tan B (2013) Nanofibers Reinforced Polymer Composite Microstructures. In book "Advances in Nanofibers" (Editor Russell Maguire), ISBN 978-953-51-1209-9, Publisher: InTech, DOI: 10.5772/45983.
23. Boeger L, Wichman MHG, Meyer LO, Schulte K (2008) Load and health monitoring in glass fibre reinforced composites with an electrically conductive nanocomposite epoxy matrix. *Comp Sci Technol* 68:1886–1894.
24. Schulte K, Baron Ch (1989) Load and failure analyses of CFRP laminates by means of electrical resistivity measurements. *Comp Sci Technol* 36:63–76.
25. Gojny FH, Wichmann MHG, Fiedler B, Kinloch IA, Bauhofer W, Windle AH, Schulte K (2006) Evaluation and identification of electrical and thermal conduction mechanisms in carbon nanotube/epoxy composites. *Polymer* 47:2036–2045.
26. Thostenson ET, Chou TW (2008) Real-time in situ sensing of damage evolution in advanced fiber composites using carbon nanotube networks. *Nanotechnology* 19:215713.
27. Nitodas S, Alexopoulos ND, Marioli-Riga Z (2010) An effective route for the functionalization/dispersion of carbon nanotubes in polymer composites for transport applications. 6th International Congress for Composites (Composites in Automotive & Aerospace), Munich, Germany, October, 2010.
28. Favvas EP, Nitodas SF, Stefanopoulos A, Stefanopoulos KL, Papageorgiou SK, Mitropoulos ACh (2014) High Purity Multi-Walled Carbon Nanotubes: Preparation, Characterization and Performance as Filler Materials in co-polyimide Hollow Fiber Membranes. *Separ Purif Technol* 122: 262–269.
29. Favvas EP, Stefanopoulos KL, Nolan JW, Papageorgiou SK, Mitropoulos ACh, Lairez D (2014) Mixed Matrix Hollow Fiber Membranes with enhanced gas permeation properties. *Separ Purif Technol* 132:336–345.
30. Zhou O, Fleming RM, Murphy DW, Chen CH, Haddon RC, Ramirez AP, Glarum SH (1994) Defects in Carbon Nanostructures. *Science* 263:1744–1747.
31. Chen P, Wu X, Sun X, Lin J, Li W, Tan KL (1999) Electronic Structure and Optical Limiting Behavior of Carbon Nanotubes. *Phys Rev Lett* 82:2548–2551.
32. Zhang HB, Lin GD, Zhou ZH, Dong X, Chen T (2002) Raman spectra of MWCNTs and MWCNT-based H2-adsorbing system. *Carbon* 40:2429–2436.
33. Zhao T, Hou C, Zhang H, Zhu R, She S, Wang J, Li T, Liu Z, Wei B (2014) Electromagnetic Wave Absorbing Properties of Amorphous Carbon Nanotubes. *Sci Rep* 4:5619.
34. Su J, Lua AC (2007) Effects of carbonisation atmosphere on the structural characteristics and transport properties of carbon membranes prepared from Kapton® polyimide. *J Membr Sci* 305:263–270.
35. Yar M, Shahzad S, Siddiqi SA, Mahmood N, Rauf A, Anwar MS, Chaudhry AA, Rehman I (2015) Triethyl orthoformate mediated a novel crosslinking method for the preparation of hydrogels for tissue engineering applications: characterization and in vitro cytocompatibility analysis. *Mater Sci Engin C* 56:154–164.